Cooling by Spontaneous Decay of Highly Excited Antihydrogen Atoms in Magnetic Traps

T. Pohl,[1] H. R. Sadeghpour,[1] Y. Nagata,[2,3] and Y. Yamazaki[2,3]

[1]*ITAMP, Harvard-Smithsonian Center for Astrophysics, 60 Garden Street, Cambridge Massachusetts 02138, USA*
[2]*Institute of Physics, University of Tokyo, 3-8-1 Komaba, Meguro-ku, Tokyo, 153-8902, Japan*
[3]*Atomic Physics Laboratory, RIKEN, Saitama 351-0198, Japan*

(Received 15 September 2006; published 22 November 2006)

An efficient cooling mechanism of magnetically trapped, highly excited antihydrogen ($\bar{\mathrm{H}}$) atoms is presented. This cooling, in addition to the expected evaporative cooling, results in trapping of a large number of $\bar{\mathrm{H}}$ atoms in the ground state. It is found that the final fraction of trapped atoms is insensitive to the initial distribution of $\bar{\mathrm{H}}$ magnetic quantum numbers. Expressions are derived for the cooling efficiency, demonstrating that magnetic quadrupole (cusp) traps provide stronger cooling than higher order magnetic multipoles. The final temperature of $\bar{\mathrm{H}}$ confined in a cusp trap is shown to depend as $\sim 2.2 T_{n_0} n_0^{-2/3}$ on the initial Rydberg level n_0 and temperature T_{n_0}.

DOI: 10.1103/PhysRevLett.97.213001 PACS numbers: 32.80.Pj, 32.60.+i, 32.70.Cs, 36.10.−k

Evaporative cooling—the process of removal of hot particles from an ensemble, necessarily leaving behind colder particles—is *the* workhorse of nearly all Bose condensation experiments. For atomic hydrogen, however, evaporative cooling is inefficient, owning to the anomalously small s-wave collision scattering length [1].

This poses serious challenges for ongoing endeavors in trapping and cooling of antihydrogen, to ultimately realize comparative, high precision spectroscopy of $\bar{\mathrm{H}}$ and H atoms. In a series of spectacular experiments, two groups [2,3] have demonstrated the formation of weakly bound Rydberg $\bar{\mathrm{H}}$ atoms in nested Penning traps. Next generation experiments aim at magnetic trapping of the atoms to provide sufficient time for radiative decay to the $\bar{\mathrm{H}}$ ground state. During this process, the effective trap depth seen by the atoms typically decreases by more than an order of magnitude, due to the drastic decrease of $\bar{\mathrm{H}}$ magnetic moments. Given the anticipated low $\bar{\mathrm{H}}$ densities ($\ll 10^7$ cm^{-3}) atom-atom collisions are negligible on the time scale of the cascade ($\approx$100 ms). Hence, evaporation proceeds without elastic collisions, which is discouraging, since all the atoms are lost from the trap before reaching the ground state.

We identify an additional, radiative decay-induced cooling mechanism (DIC), which dominates over evaporative cooling and allows for a considerable fraction of ground state $\bar{\mathrm{H}}$ atoms, to be trapped in achievable magnetic fields. Since the fraction of low-field seeking (LFS) atoms, those with $+m$ projection, is nominally small [4], efficient trapping of $\bar{\mathrm{H}}$ represents a top priority.

In evaporative cooling schemes, hot atoms are lost through spillage over the top of the trap and, more importantly, by elastic *two-particle* collisions, as the trap depth is decreased, e.g., by a "rf scalpel" [5] [Fig. 1(a)]. In contrast, DIC is a *single-particle* process, due to decreasing internal energy, as the atomic magnetic moment decreases in the course of the radiative cascade in the inhomogeneous magnetic field $B(\mathbf{r}) = |\mathbf{B}(\mathbf{r})|$ [Fig. 1(b)].

It is not at all clear if sufficient cooling can be achieved and to what extent atom loss is sustainable. Moreover, the field cannot be considered as a perturbation, raising the question of how the strong magnetization of the atoms, and hence the trap geometry affects the cooling process. Here, we address these questions and perform feasibility studies for future $\bar{\mathrm{H}}$ trapping experiments.

In the presence of a strong magnetic field, the hydrogenic quantum numbers $\boldsymbol{\eta} = (n, l, m, s)$ are no longer good quantum numbers. Nevertheless, we will use them to label the atomic state, connected to the field-free state (n, l, m, s) as B is decreased to zero. Hence, the $\bar{\mathrm{H}}$ states are completely determined by (n, l, m, s) and B, such that the external potential $U_{\boldsymbol{\eta}}$ can be written as

$$U_{n,l,m}(\mathbf{r}) = \mu[n, l, m, s, B(\mathbf{r})]B(\mathbf{r}). \quad (1)$$

To determine the magnetic moment μ, we ignore the spin-

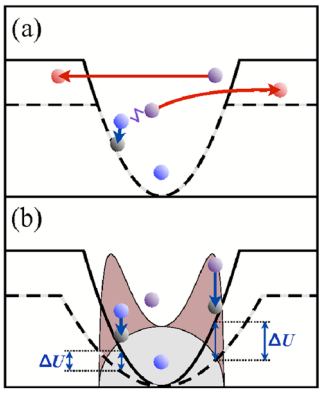

FIG. 1 (color online). Gas dynamics due to a changing external potential (from solid to dashed lines). The standard evaporative cooling is shown in (a). In (b), the decreasing potential energy of trapped atoms, results in collisionless cooling during the radiative cascade of Rydberg atoms. The shaded areas indicate the distribution of decay events under the assumption of field-free $\bar{\mathrm{H}}$s (light area) and accounting for magnetic field effects (dark area). DIC is more efficient in the latter case.

orbit coupling (Paschen-Back regime), as appropriate either for large n or for $n = 1$. Since the $\bar{H}$ spend a short time in intermediate levels $1 < n < 10$, this approximation does not affect the center-of-mass (COM) dynamics.

There are different proposals for simultaneous trapping of opposite charges and neutral $\bar{H}$ atoms. In the case of a nested Penning trap for $\bar{H}$ production, it has been recently demonstrated [6] that higher order magnetic multipoles should be used to confine $\bar{H}$ atoms, to reduce ballistic charge transport into the walls. Another working proposal is to use a magnetic cusp trap combined with an electric octupole field [7], to simultaneously confine antiprotons ($\bar{p}$), positrons (e^+), and $\bar{H}$ in the same spatial region [8], while allowing large magnetic field gradients without jeopardizing the plasma confinement. This setup also has the advantage of producing thermal $\bar{p}$, and hence thermal $\bar{H}$. Here, we will mainly focus on the cusp configuration, but also give a more general, analytical discussion of the cooling efficiency in higher order multipole traps.

While spectral properties of strongly magnetized Rydberg atoms (see, e.g., [9]) have been extensively studied in the past, spontaneous decay and trapping of Rydberg atoms in strong magnetic fields has attracted interest only recently [10–12]. Here we account for the strong B field, by numerically diagonalizing the Hamiltonian for a frozen $\bar{H}$ atom in a homogeneous magnetic field, to obtain atomic binding energies, magnetic moments, and radiative transition rates for all states below $n \leq 45$ and $0 \leq B \leq 4$ T. This approach neglects the motional Stark effect [13] and assumes adiabatic alignment of the $\bar{H}$ magnetic moment along the field lines, both justified for the considered parameters.

The calculations show that the magnetic field reduces the decay rate for negative m states but enhances the rate for $m > 0$ (see also [10,11]). For circular Rydberg states, this behavior is readily understood in the low-field limit, where the binding energies are shifted due to the linear Zeeman term while the transition matrix elements remain unaltered. The field-dependent decay rate

$$\Gamma^m_{m\mp1}(B) = \left(1 \pm \frac{n'^2}{n + n'} \frac{\mu_B B}{\varepsilon_n}\right)^3 \Gamma^m_{m\mp1}(B = 0), \quad (2)$$

is enhanced for $0 < m \rightarrow m - 1$ transitions and vice versa, where $\varepsilon_n = -13.6\ \mathrm{eV}/n^2$ is the field-free binding energy.

Having calculated the transition frequencies, magnetic moments, and oscillator strengths, we determine the atomic phase space distribution $f(\mathbf{r}, \mathbf{v}, \boldsymbol{\eta}, t)$ from the kinetic equation

$$\left(\frac{\partial}{\partial t} + \mathbf{v}\frac{\partial}{\partial \mathbf{r}} + \frac{\partial U_{\boldsymbol{\eta}}(\mathbf{r})}{\partial \mathbf{r}}\frac{\partial}{\partial \mathbf{v}}\right) f(\mathbf{r}, \mathbf{v}, \boldsymbol{\eta}, t) = \sum_{\boldsymbol{\eta}'} \Gamma^{\boldsymbol{\eta}'}_{\boldsymbol{\eta}} f(\mathbf{r}, \mathbf{v}, \boldsymbol{\eta}', t) - \Gamma^{\boldsymbol{\eta}}_{\boldsymbol{\eta}'} f(\mathbf{r}, \mathbf{v}, \boldsymbol{\eta}, t), \quad (3)$$

where $\Gamma^{\boldsymbol{\eta}}_{\boldsymbol{\eta}'}$ is the rate of radiative transition from $\boldsymbol{\eta}$ to $\boldsymbol{\eta}'$, and $\mathbf{r}$ and $\mathbf{v}$ are the atomic position and velocity, respectively. For a given initial internal state distribution $\varphi_0(\boldsymbol{\eta})$, the simulation starts from a thermal COM distribution

$$f(\mathbf{r}, \mathbf{v}, \boldsymbol{\eta}, 0) \propto \exp\left(-\frac{Mv^2}{2k_B T(0)} - \frac{U_{\boldsymbol{\eta}}(\mathbf{r})}{k_B T(0)}\right)\varphi_0(\boldsymbol{\eta}), \quad (4)$$

where k_B denotes the Boltzmann constant and M is the $\bar{H}$ mass. We typically choose fixed values of $n = n_0$ and $m = m_0$, while randomly sampling $m_0 \leq l_0 < n_0$.

Figure 2 displays the essential features of our calculations. The temporal dynamics of the number of trapped atoms and the resulting cooling are shown in Figs. 2(a) and 2(b), starting from an initially circular Rydberg state with $n_0 = 44$ and an initial temperature of $T(0) = 15$ K. The kinetic energy decreases by about a factor 40 with a well-fitted Maxwellian distribution, even in the absence of atom-atom collisions. We also calculate the accumulated energy loss ΔE_{DIC} and ΔE_{evap}, due to DIC and evaporation, respectively. DIC is found to dominate over evaporative cooling in removing energy from the system [Fig. 2(c)], resulting in a significant fraction of trapped $\bar{H}$. We note that the final fraction of trapped atoms decreases as $\sim T(0)^{-1.6}$ for 10 K $\leq T(0) \leq$ 30 K.

The trapping efficiency, however, also depends on the orientation of the e^+ spin, as the only remaining magnetic moment in the ground state. The two curves in Figs. 2(a) and 2(b) are calculated by assuming 100% LFS ground

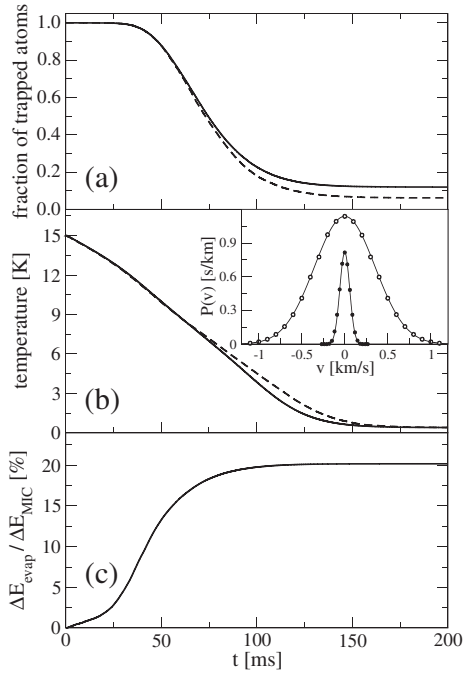

FIG. 2. Time evolution of the number of trapped atoms (a) and the atomic temperature (b) for $n_0 = 44$, $m_0 = 43$. The solid and dashed curves refer to 100% low-field seeking ground state atoms and an equal mixture of e^+ spin orientations, respectively. The inset shows the initial (open circles) and final (closed circles) velocity distribution fitted to Maxwellian curves with temperatures $T(0) = 15$ K and $T(\infty) = 0.4$ K, respectively. The cusp trap has a B-field difference of 4 T. (c) Ratio of energy loss due to evaporation and DIC.

state atoms and by randomly sampling the orientation of the e^+ spin. Since the gas dynamics is collisionless, the mixing ratio of positive and negative e^+ spins does not affect the final temperature but is directly proportional to the final fraction of trapped atoms. $\bar{H}$ atoms with $s = -1/2$ that are ejected from the cusp trap after reaching the ground state (high-field seekers), are essential for precise $\bar{H}$ hyperfine transition measurements proposed in [7]. In the following we choose all e^+ spins to be oriented along the magnetic field. Different spin mixtures can be accounted for by multiplying the final fractions with the respective relative number of positive spin states.

The atomic state distribution in both ATHENA [2] and ATRAP [3] experiments is not yet known completely. Recently, it was shown that the probability of binding energies E_b in the ATRAP setup decreases as E_b^{-5} [14]. Moreover, Monte Carlo simulations indicate that a small fraction of LFS ($\mu > 0$) $\bar{H}$ are formed [4], while the precise distribution of magnetic moments under experimental conditions remains unknown. In view of these uncertainties, we undertook a broad parameter scan, exemplified in Fig. 3. In Fig. 3(a), we show the trapping efficiency for fixed $n_0 = 44$ and varying m_0. To avoid loss of $\bar{H}$ in the initial states, we limit ourselves to $m_0 > 32$. In this range, decreasing m_0 accelerates the atom loss, but leaves the final fraction of trapped atoms unchanged. When plotted against the average principal quantum number $\langle n \rangle$, the results collapse on a single curve. This insensitivity to m_0 is due to the fact that the $\bar{H}$ atom is quickly driven to a circular Rydberg state during the cascade [15]. Precise knowledge of the m_0 distribution of *initially confined states* is therefore not crucially important for $\bar{H}$ trapping experiments

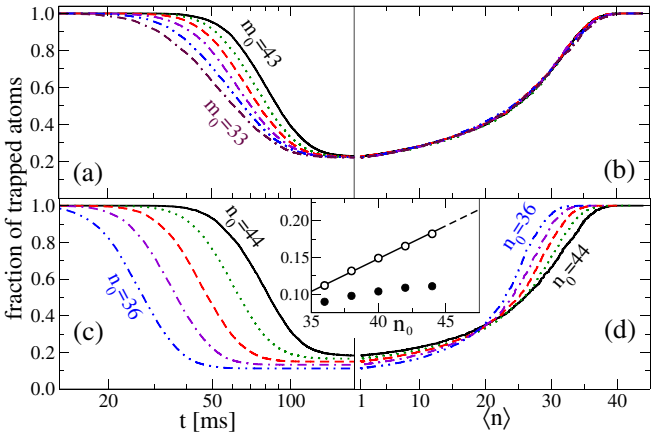

FIG. 3 (color online). Fraction of trapped atoms as functions of time [(a),(c)] and average principal quantum number [(b),(d)], for $n_0 = 44$ and different initial $33 \leq m_0 \leq 43$ [in (a) and (b) at $T(0) = 10$ K] and circular Rydberg atoms with $36 \leq n_0 \leq 44$ [in (c) and (d) at $T(0) = 12$ K]. Different curves are steps of two in m_0 and n_0. The inset shows the linear n_0 dependence of the fraction of trapped atoms (open circles), which disappears when strong magnetic field effects are neglected (closed circles). The trap parameters are identical to Fig. 2.

and the ensuing discussion can safely be restricted to the simpler case of circular Rydberg states.

The trapping efficiency, on the other hand, is affected by n_0. While the final temperature is independent of n_0, DIC becomes more efficient for larger n_0, as less atoms evaporate during the cascade [see Figs. 3(c) and 3(d)]. There is a clear linear increase of the number of trapped atoms with increasing n_0, largely a consequence of field effects on the atomic state.

Two mechanisms conspire to enhance the cooling efficiency in the magnetic traps. First, the radiative decay rate increases with increasing B such that it is peaked at the edges of the trap, where the change in potential energy, and therefore the cooling effect is largest [Fig. 1(a)]. Second, the quadratic Zeeman shift leads to a larger energy loss as the atoms decay to a lower state at the outer regions of the trap. Both of these effects enhance the number of trapped atoms compared to the expected dynamics in a weak magnetic field. An independent calculation of the radiative cascade, neglecting both of these effects, finds a reduction of the atomic translational energy [16].

While the preceding numerical discussion was focused on the cusp trap geometry [7], we now give analytical arguments in support of our prediction that DIC of Rydberg atoms has universal appeal. We begin by considering a spherically symmetric field $B = \beta(r/\lambda)^\gamma$, with $\gamma = 1$ corresponding to the cusp trap case, and larger values of γ reproducing the central trap shape of higher order multipole fields. Furthermore, we neglect the diamagnetic term in the Hamiltonian, such that the external potential of circular states is given by $U_n = \mu_B n B$. An atom in state n with a total COM energy $E_n = K_n + U_n$, decaying at position $\mathbf{r}_0$ to a lower lying state n' therefore loses energy $\mu_B(n' - n)B$, to be redistributed among its potential and kinetic energy. Upon using the virial theorem, we obtain for the final average kinetic energy

$$\langle K_{n'} \rangle = \langle K_n \rangle - \frac{\gamma}{2+\gamma}\left(\frac{n-n'}{n}\right) U_n(r_0). \qquad (5)$$

Finally, the average change in kinetic energy is obtained from an ensemble average, i.e., from averaging over $\mathbf{r}_0$ according to the distribution of radiative decay events.

First consider the case of n sufficiently low for radiative decay to the ground state to be much faster than the time scale on which the atom moves. In this case the position dependence of the transition rate is unimportant and we can once more employ the virial theorem $\langle U(r_0) \rangle = 2\langle K_n \rangle/\gamma$ to obtain for the temperature T_n

$$T_1 = \frac{n\gamma + 2}{n(\gamma + 2)} T_n. \qquad (6)$$

Hence, cooling during the sudden cascade to the ground state becomes inefficient in higher order potentials [Fig. 4(b)] and is optimal for the cusp trap [Fig. 4(a)].

In the opposite limit of radiative decay proceeding slowly compared to the time scale of the COM motion,

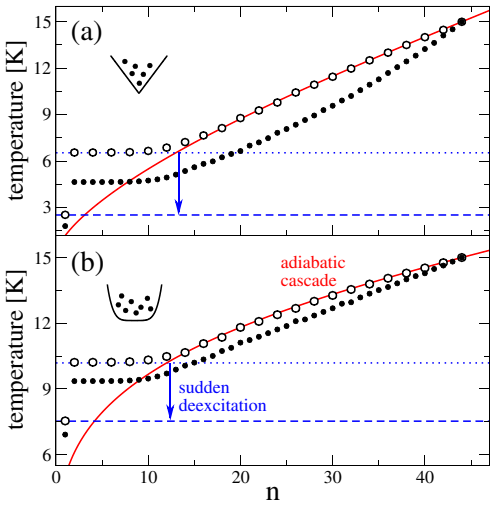

FIG. 4 (color online). n dependence of the atomic temperature of circular Rydberg states for $n_0 = 44$, $T(0) = 15$ K, $\gamma = 1$ (a), and $\gamma = 5$ (b). The open circles show the numerical results neglecting the diamagnetic term in the atomic Hamiltonian, and the closed circles result from the full calculations. The solid line is obtained for the adiabatic cascade from Eq. (8), while the dotted and dashed lines indicate the temperature decrease due to the sudden deexcitation according to Eq. (6).

the temperature decreases in consecutive steps according to Eq. (5) and we have to account for the position dependence of the transition rate according to Eq. (2). After performing the ensemble average and in the limit $(n - n')/n \to 0$, we obtain the following differential equation for the temperature, up to first order in T_n/ε_n

$$\frac{dT}{dn} = \left(2 + \frac{9\langle \delta U^2 \rangle}{\gamma}\frac{T}{\varepsilon_n}\right)\frac{T}{(2+\gamma)n}, \tag{7}$$

where $\langle \delta U^2 \rangle = \frac{\langle U^2 \rangle - \langle U \rangle^2}{\langle U \rangle^2} = \frac{\gamma 2}{5\gamma + 6}$. Equation (7) permits a simple and instructive solution

$$T_n = \frac{T_{n_0}\left(\frac{n}{n_0}\right)^{2/(2+\gamma)}}{1 + \kappa\left[1 - \left(\frac{n}{n_0}\right)^{(2\gamma+6)/(\gamma+2)}\right]}, \tag{8}$$

with $\kappa = \frac{9\gamma}{2(5\gamma+6)(\gamma+3)}\frac{k_B T_{n_0}}{\varepsilon_{n_0}}$, revealing an approximate power-law cooling $\propto n^{2/(2+\gamma)}$, which is enhanced by magnetic field effects since $\kappa > 0$. Again, cooling becomes less efficient with increasing multipole order. Figure 4 shows the numerically calculated temperature $k_B T_n = \frac{M}{3} \times \int v^2 f(r, v, n, t) d\mathbf{r} d\mathbf{v} dt$. The two cooling regimes, i.e., the adiabatic cascade followed by a sudden deexcitation, can clearly be identified. Moreover, the approximate simulations nicely follow the analytical predictions.

With the crossover occurring at $10 < n_c < 15$, Eqs. (6) and (8) yield a simple expression for the final temperature at not too large magnetic fields ($\kappa \approx 0$)

$$T_1 \approx \frac{n_c \gamma + 2}{n_c(\gamma + 2)}\left(\frac{n_c}{n_0}\right)^{2/(2+\gamma)} T_{n_0}, \tag{9}$$

which for a cusp trap and $n_c \approx 13$ gives $T_1 \sim 2.2 T_{n_0} n_0^{-2/3}$. The full simulations predict stronger cooling due to the diamagnetic term in the atomic Hamiltonian, whose influence becomes less pronounced as γ increases. Thus, particularly, for higher order multipole traps, Eq. (9) provides valuable estimates for future $\bar{H}$ trapping schemes.

In conclusion, we have revealed an efficient cooling mechanism by spontaneous decay, present in strong magnetic field traps of Rydberg atoms. As this additional cooling largely reduces atom loss, it holds promise for future $\bar{H}$ trapping experiments. We identified two distinct cooling stages—an adiabatic cascade cooling followed by sudden deexcitation —showing a strong dependence on the multipole order of the field configuration and favoring lower order traps. While the trapping efficiency is independent of the initial magnetic quantum number, it increases with increasing initial excitation energy. We finally note, that state-changing $e^+ -$ and $\bar{p} - \bar{H}$ collisions could lead to additional loss of highly excited atoms, which may require spatial separation of the trapped $\bar{H}$ from the production region. The importance of collisions with magnetized, large $+m$ Rydberg atoms, hence constitutes an open question for future $\bar{H}$ studies.

This work was supported by NSF through a grant for ITAMP. T. P. and H. R. S. are grateful to NSF/INT-0300708 for travel to Japan, where this work was initiated.

[1] M. J. Jamieson, A. Dalgarno, and M. Kimura, Phys. Rev. A **51**, 2626 (1995).
[2] M. Amoretti *et al.*, Nature (London) **419**, 456 (2002).
[3] G. Gabrielse *et al.*, Phys. Rev. Lett. **89**, 213401 (2002); **89**, 233401 (2002).
[4] F. Robicheaux, Phys. Rev. A **73**, 033401 (2006).
[5] M. H. Anderson *et al.*, Science **269**, 198 (1995).
[6] J. Fajans *et al.*, Phys. Rev. Lett. **95**, 155001 (2005).
[7] A. Mohri and Y. Yamazaki, Europhys. Lett. **63**, 207 (2003).
[8] Atom loss due to Majorana spin-flip transitions in the cusp trap is not a serious problem as discussed in [7].
[9] C. H. Iu *et al.*, Phys. Rev. Lett. **66**, 145 (1991).
[10] J. R. Guest, J.-H. Choi, and G. Raithel, Phys. Rev. A **68**, 022509 (2003).
[11] T. Topcu and F. Robicheaux, Phys. Rev. A **73**, 043405 (2006).
[12] J.-H. Choi *et al.*, Phys. Rev. Lett. **95**, 243001 (2005).
[13] P. Schmelcher and L. S. Cederbaum, Phys. Rev. A **47**, 2634 (1993).
[14] T. Pohl, H. R. Sadeghpour, and G. Gabrielse, Phys. Rev. Lett. **97**, 143401 (2006).
[15] M. R. Flannery and D. Vrinceanu, Phys. Rev. A **68**, 030502(R) (2003).
[16] C. L. Taylor, J. Zhang, and F. Robicheaux, J. Phys. B **39**, 4945 (2006).